Journal of Catalysis **185,** 272–285 (1999)
Article ID jcat.1999.2487, available online at http://www.idealibrary.com on IDEAL®

Influence of Fine Structural Characteristics of VPO Catalysts on the Formation of Maleic and Phthalic Anhydrides in the Oxidation of *n*-Pentane

Z. Sobalik,[1] S. Gonzalez Carrazan, P. Ruiz, and B. Delmon

Unité de Catalyse et Chimie des Matériaux Divisés, Université Catholique de Louvain, Place Croix du Sud 2/17, B-1348 Louvain-la-Neuve, Belgium

Received May 18, 1998; revised February 5, 1999; accepted March 1, 1999

We report on the influence of the stages of preparation of a vanadium phosphate on the selectivity to phthalic anhydride (PA) and maleic anhydride (MA) in *n*-pentane oxidation. The attention was mainly focused on the extent of structural defects observed in precursors and catalysts. Vanadium phosphate catalysts were obtained from precursors prepared by a two-step synthesis. In the first step $VOPO_4$-mixed isobutanol–water intercalates, with the amount of isobutanol per $VOPO_4$ molecule varying from 1.6 to 0.05, were prepared by precipitation from a solution containing vanadyl isobutoxide and H_3PO_4 and a carefully adjusted water content. In the second step the precursors were formed by reflux using two different procedures: (i) in an inert medium (*n*-octane) or (ii) in a reductive medium (isobutanol). Catalysts were obtained by treating the precursors under the reaction conditions for about 40 h. By such procedures VPO precursors and catalysts with bulk P/V atomic ratio equal to 1.05 and displaying widely different structural defects were obtained. Precursors and catalysts were characterised by elementary chemical analysis, carbon analysis, oxidation state of vanadium, BET, XRD, FTIR, and XPS. Long range and short range orders were considered. Results show that the parallel routes of the *n*-pentane oxidation into MA and PA require different structural features of the catalyst. The formation of phthalic anhydride demands an ordered structure while maleic anhydride could be formed on a highly defective VPO catalyst. It is suggested that this high structural order for PA formation is necessary to create the complex active structure to provide the concerted process of PA formation. © 1999 Academic Press

Key Words: **phosphous vanadium catalyst; *n*-pentane; maleic and phthalic anhydrides.**

INTRODUCTION

The oxidation of *n*-pentane over vanadium phosphate catalysts constitutes an interesting subject of study for practical and fundamental reasons. This reaction gives relatively large amounts of phthalic anhydride (PA) in addition to maleic anhydride (MA), this implying the condensation of two *n*-pentane molecules and the complete oxidation of two carbon atoms per PA molecule formed. The occurrence of this complicated reaction raises fundamental questions concerning the mechanisms operating in oxidation. The practical aspects of this reaction were discussed previously by Centi *et al.* (1). They concluded that a substantial increase of selectivity to phthalic anhydride is absolutely necessary if future industrial applications are contemplated.

The formation of PA by oxidation of *n*-pentane requires a complicated set of connected reactions which must be realised without disrupting the structure of the catalyst, thus suggesting the existence of a very complex set of active sites with a precise surface topology, the possibility of an exact timing of the consecutive steps, and an easy desorption of the final product. Another problem is the difficulty of increasing the overall selectivity in valuable products (PA and MA). The system seems to exhibit a strong tendency to overoxidation, thus leading to still more total oxidation products (2).

Only a limited number of articles can be found in the literature concerning the dependence of the catalytic performances on the solid state properties of VPO catalysts. The problem of *n*-pentane oxidation into PA was recently analysed by Cavani *et al.* showing the role of VPO surface properties (3, 4) and Co and Fe addition (5). In butane oxidation to MA, Ebner *et al.* (6) concluded that the surface topology of VPO catalysts allowing PA or MA formation should correspond to a tridimensional surface structure. It is most likely constituted of surface cavities involving vacancies of two adjacent pyrophosphate groups, with the vanadyl groups situated at the bottom of the cavities. As suggested by Centi (7), the shape and size of these or similar tridimensional structures may control the ratio of MA and PA formation in *n*-pentane oxidation on vanadyl phosphate catalysts. If we admit this view, it could be further speculated that some features of such complex surface structures are influenced by the structural order of the surface and subsurface layers of a VPO catalyst. However, an experimental support for such conclusions has not been presented yet in the literature.

[1] Present address: J. Heyrovsky Institute of Physical Chemistry, Academy of Sciences of the Czech Republic, Dolejskova 3, 182 23 Prague 8, Czech Republic.

0021-9517/99 $30.00

It is therefore desirable to re-examine the role of these surface structures and their relations to the underlying structure in relation to their behaviour in *n*-pentane oxidation. Due to the complexity of the catalyst precursors and final catalysts, it is very likely that the catalytic performances of VPO catalysts depend directly on the preparation method and more specifically on certain critical experimental parameters during this preparation.

In a previous work (8) we have shown that the control of the formation of the precursor is crucial for obtaining a selective VPO catalyst. It was shown that the formation of PA is favoured by a well-crystallized $(VO)_2P_2O_7$ phase with minor formation of defects, which was obtained in this case from the $VOHPO_4 \cdot 1/2H_2O$ precursor via $VOPO_4 \cdot 2H_2O$ phase in a mixed water–isobutanol media. Nevertheless the P/V value in the precursors in this study also differed and that made the interpretation of our previous results more complex (8). A similar conclusion has been recently presented by Albonetti *et al.* (9), suggesting that only a well-crystallised phase of $(VO)_2P_2O_7$, formed in his experiments during prolonged *in situ* equilibration, provides the geometric features necessary for the conversion of *n*-pentane into PA.

The objective of this paper is to study more in detail the influence of the addition of water on the properties of the precursors and correlate their corresponding solid state properties with their catalytic activity in *n*-pentane oxidation and in particular with the selectivity to MA and PA. There is also a practical aspect of this problem, as water always constitutes a component of the preparation mixture even in the so-called "organic medium" preparation route, where it is formed by alcoholysis of V_2O_5 by reaction with alcohol used as a solvent.

The approach we followed in this work was the following:

(1) to prepare an alcohol intercalated VPO precursor and separate it from the preparation solvent initially containing various amounts of alcohol and water,

(2) to introduce this intercalated precursor in two different media: either an inert medium (*n*-octane) or a reductive medium (isobutanol). We used *n*-octane as a nonreductive medium having a boiling temperature similar to that of isobutanol, thus allowing us to use a similar temperature in the next preparation step under reflux. The objective of this procedure was to determine the reductive effect of isobutanol intercalated in the precursor. All samples were prepared with a nearly constant P/V bulk ratio.

Precursors and catalysts were characterised by various physico-chemical techniques: elementary chemical analysis, carbon analysis, oxidation state of vanadium BET, XRD, FTIR, and XPS. The amount of alcohol in the VPO precursor has been calculated taking into account the amount of carbon analysed by elementary analysis.

The catalytic activity was studied in the oxidation of *n*-pentane to MA and PA. This was measured after a relatively short activation period (compared to, e.g., 200 hours suggested by Albonetti *et al.* (9) for full equilibration). Under these conditions, it was expected that the structural features characteristic of the individual $VOHPO_4 \cdot 1/2H_2O$-type precursors and, namely the level of the structural defects, would be transcribed into structural parameters of the individual catalysts and preserved during the short catalytical test (compared to, e.g., (10–12)), allowing us to correlate structural characteristics of both the precursor and the catalyst with the catalytic performances.

EXPERIMENTAL

(a) Materials

V_2O_5 (Janssen Chimica, purity >99.9%), isobutanol (Aldrich; by Karl Fisher titration, the content of water was found to be 0.1%), H_3PO_4 (Fluka, purity >99%), benzene (Aldrich, purity >99%), and *n*-octane used for VPO preparation (Aldrich, purity >99%) were used as delivered by the manufacturer. Water was purified on a Milli-Q plus system, SiC (particle size 0.3 mm) provided by Prolabo was used as delivered.

(b) Preparation of Vanadyl Isobutoxide

Vanadyl isobutoxide was prepared by refluxing 40 g of V_2O_5 in 500 ml of isobutanol with the addition of 50 g of benzene (13). The water formed during the alcoholysis was continuously removed in the form of the water–benzene azeotrope and separated in a Dean–Stark apparatus. After refluxing for about 40 h the rest of the unreacted V_2O_5 was filtered out using a membrane filter <0.2 mm (Schleicher & Schuele 100) and the solvent was evaporated at 50°C at a lower pressure (about 12 Torr) for 16 h. The vanadium content found in the product was about 95% of the theoretical value expected for pure vanadyl isobutoxide.

(c) Catalyst Precursors Preparation

The preparation procedure is depicted in a simplified way in Fig. 1.

Precursor A

(i) Preparation of vanadyl isobutoxide solution in water–isobutanol. First, 11.44 g of vanadyl isobutoxide solution (0.04 mole) was added under vigorous stirring to a 100 ml of water–isobutanol solution at room temperature. The amounts of water used in the preparation are indicated in Table 1. In preparations with higher amounts of water (5, 6, and 7) the starting solution was identical (namely containing only 1.6 g of water), and the rest was added during the subsequent preparation step (see section (ii)).

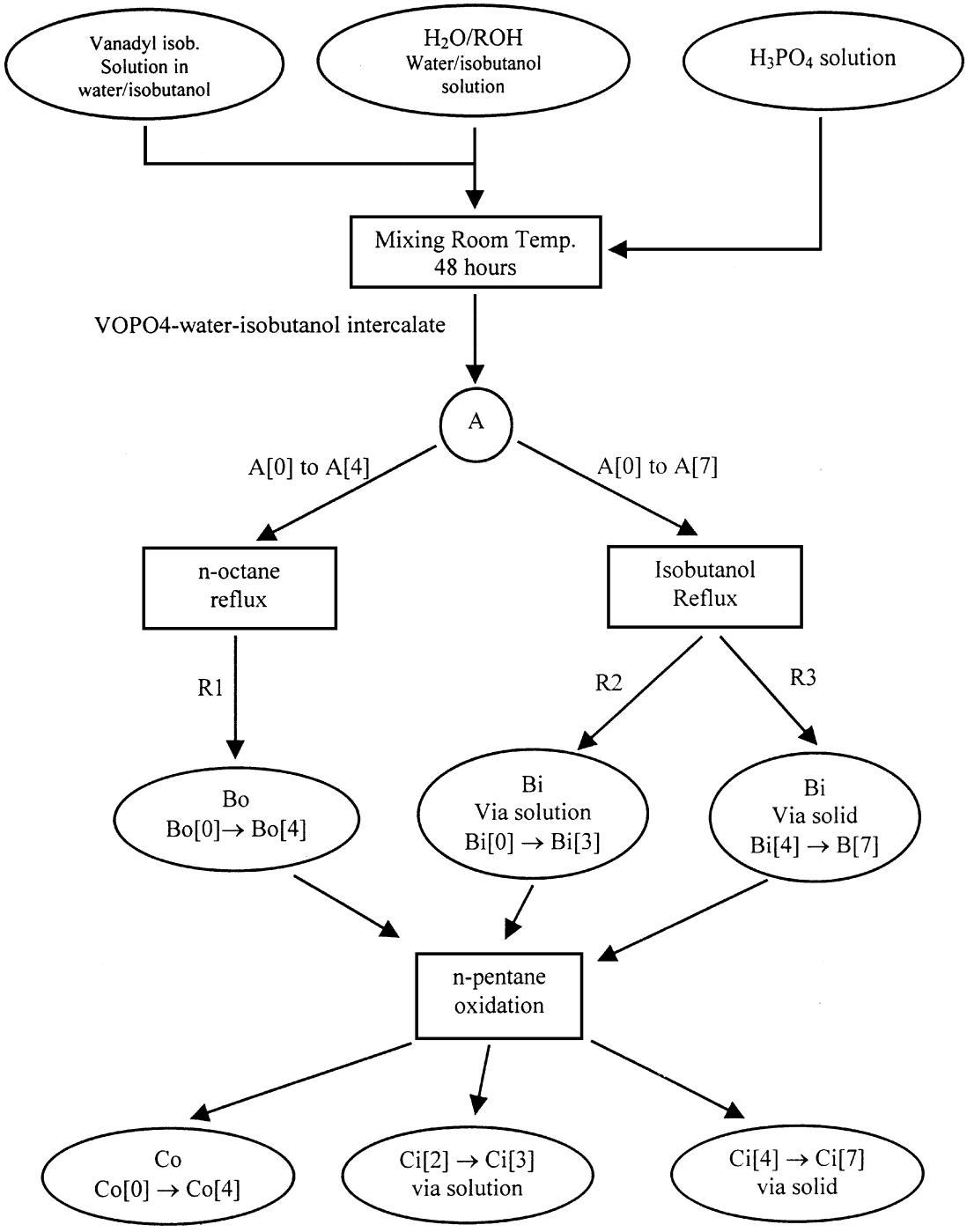

FIG. 1. Scheme of samples preparation. R1, solid state reduction in inert media (*n* octane); R2, reduction via solution in isobutanol media; R3, reduction via solid in isobutanol media.

(ii) Precursor precipitation. First, 3.92 g of H_3PO_4 (0.04 mole) dissolved in 50 ml of isobutanol were slowly added under vigorous stirring at room temperature to the vanadyl isobutoxide solution in the water/isobutanol mixture. Then the amount of water was adjusted by adding the rest of the water (see Table 1) and the mixture was stirred for another 48 h. After that time, the solid was isolated by filtration and dried for 2 h in a vacuum oven (about 12 Torr) at 50°C. The samples were denoted as Precursors A[0] to A[7].

Precursor Bo

Only precursors A[0] to A[4] were used for this preparation. First, 5.5 g of precursor A were dispersed in 100 ml of *n*-octane and stirred at room temperature for 45 min.

TABLE 1

Characteristics of the Bulk Composition of Precursors A

Sample	A[0]	A[1]	A[2]	A[3]	A[4]	A[5]	A[6]	A[7]
Water added, g[a]	0	0.32	0.64	1.28	1.60	2.10	2.90	3.70
$(P/V)_b$	1.05	1.05	1.03	1.01	1.02	1.03	1.03	1.02
$(C/V)_b$	6.5	4.5	4.0	2.6	2.1	1.1	0.64	0.2
n	1.62	1.12	1.0	0.65	0.53	0.27	0.21	0.05
V^{n+}, bulk	5.0	5.0	5.0	5.0	4.8	4.8	4.8	4.8

Note. n is the number of isobutanol molecules per $VOPO_4$ unit as calculated using the C/V value, $(P/V)_b$ is the bulk atomic ratio of carbon and vanadium as obtained by chemical analysis, $(C/V)_b$ is the bulk atomic ratio of carbon and vanadium as obtained by chemical analysis, and V^{n+} is the average oxidation state of vanadium as calculated from the results of manganometric titration and the total amount of vanadium found by ICP analysis.

[a] g of water added to 200 ml of the total amount of isobutanol in the preparation solution.

Then the temperature was increased until ebullition and the mixture was refluxed for 20 h. The solid obtained was then isolated by evaporation of the solvent in a Rotavapor under low pressure (about 12 Torr) and dried at 80°C for 18 h. The samples were denoted Precursors Bo[0] to Bo[4].

To check the behaviour of the $VOPO_4$ without any isobutanol intercalated under the reflux in an inert media, 5.5 g of $VOPO_4 \cdot 2H_2O$ were dispersed in 100 ml of *n*-octane and refluxed for 20 h. $VOPO_4 \cdot 2\ H_2O$ was prepared by mixing 12.0 g of V_2O_5 with 12.9 g of H_3PO_4 in ca. 280 ml of water at about 40°C for 40 h and isolated by solution evaporation at low pressure (about 12 Torr).

Precursor Bi

First, 5.5 g of precursor A were dispersed at room temperature in 40 ml of isobutanol, stirred for 45 min, and then the temperature was increased and the mixture refluxed for 16 h. The mixture was subsequently cooled to room temperature and the solid isolated by filtration and dried at low pressure (about 12 Torr) at 80°C for 18 h. The samples prepared were denoted precursors Bi[0] to Bi[7].

Samples C

Precursors B were pretreated under reaction conditions by a standard procedure (see catalytic test). At the end of the catalytic test, i.e., after about 40 h on stream, the reactor was cooled to room temperature in the reaction mixture and the sample was taken out. Samples prepared from precursors Bo are denoted Co and samples prepared from precursors Bi are denoted Ci.

Characterisation Methods

(i) Elemental Chemical Analysis

The determination of vanadium and phosphorus content was made by an inductively coupled plasma atomic absorption spectrometer (ICP) after dissolution of the samples in 0.1 M of nitric acid. Carbon analysis was made by measuring the amount of CO_2 produced by total oxidation using a Coulomat 702 (Stroehlein).

(ii) Oxidation State of Vanadium

About 50 mg of the solid were dissolved in 200 ml of a 2 M H_2SO_4 solution at about 60°C, and then the solution was cooled to room temperature and titrated by ca. 0.1 N $KMnO_4$. For the determination of the average oxidation state of vanadium, this result was compared to the total amount of vanadium as determined by the ICP analysis.

(iii) Specific Surface Area and Pore Distribution

The BET specific surface area and the pore distribution were obtained using ASPAP 2000 (Micromeritics) N_2 adsorption at −196°C. Pore distribution was evaluated using pore volume/pore diameter plots. Before adsorption, the samples were degassed at 125°C for 3 h.

(iv) XRD Analysis

Powder X-ray diffraction analysis was obtained in a high resolution X-ray diffractometer Siemens D-500 XRD using Cu$K\alpha$ radiation. For XRD spectra interpretation data available for $VOPO_4$ hydrates and alkoholates, i.e., for $VOPO_4 \cdot 2H_2O$ data identified by McMurdie (14), taking the most intensive peak at about $2\theta = 11.8°$ and indexed as (001), for $VOPO_4 \cdot H_2O$ data presented by Ladwing (15) taking the prominent band at $2\theta = 12°$ indexed as (001), and with the second most intensive line (002) at $2\theta = 28°$, and for $VOPO_4$-aliphatic alcohol intercalates as presented by Beneö *et al.* (16). This band shows a change in the basal spacing as a function of the intercalated alcohol: methanol (7.84 Å), ethanol (13.11 Å), *n*-propanol (14.4 Å), and *n*-butanol (17.9 Å).

The identification of XRD reflections of $VOHPO_4 \cdot 1/2H_2O$ and $(VO)_2P_2O_7$ were taken according to Bordes *et al.* (17). Accordingly, the $VOHPO_4 \cdot 1/2H_2O$ line at the $2\theta = 15.5°$ was indexed as (010) and the second prominent line at $2\theta = 30.4°$ as (202). The line of $(VO)_2P_2O_7$ at $2\theta = 23.2°$ was identified as (020) and at $2\theta = 28.3°$ as (204).

(v) Infrared Spectroscopy

FTIR spectra were recorded with a Bruker IFS 88 spectrometer at a resolution of 4 cm^{-1} using the standard KBr-technique. The observed IR bands of Precursor A were interpreted using the assignments proposed by Ladwig [15] for $VOPO_4$ mono- and dihydrates and complemented by R'Kha (18). For identification and analysis of the $VOHPO_4 \cdot 1/2H_2O$ and $(VO)_2P_2O_7$ species, assignments presented by Busca (12) were used.

(vi) X-ray Photoelectron Spectroscopy

XPS analyses were performed under ultrahigh vacuum (close to 5×10^{-9} Torr) with an SSX-100 model 206 X-ray photoelectron spectrometer from FISONS. X-rays produced by a monochromatized aluminium anode (AlKa = 1486.6 eV) were focused in an area of around 1 mm^2. The pass energy was set at 50 eV (resolution 2). In these conditions, the energy resolution (FWHM, full width at half maximum height) of Au 4f7/2 was 1.0 eV. The surface positive charge originating from the ejected photoelectrons was compensated by a "floodgun" operating at 6 eV and a nickel grid set at 3 mm above the samples. Powdered samples were located into small stainless steel troughs.

The C1s, V2p3/2, V2p1/2, O1s, P2p, and C1s bands were swept successively. The binding energy (BE) values were calculated with respect to C1s (BE of C–CH fixed at 284.8 eV). The composite V2p peaks were decomposed by the least square fitting routine provided by the spectrometer producer. In the decomposition process the Gaussian/Lorentzian ratio was 85/15, the difference in binding energies between the V2p3/2 and V2p1/2 peaks was set at 7.3 eV, and the V2p3/2/V2p1/2 intensity ratio was fixed to 2.0.

The XPS atomic ratios, P/V, C/P, and C/V, were calculated from XPS intensities by using atomic sensitivity factors provided by the spectrometer manufacturer and with respect to that of the external reference SiO_2.

For indication of the oxidation state of vanadium, BE of V2p3/2 of 518.1 eV and 517.4 eV for V^{5+} and for V^{4+} were used, respectively (19).

Catalytic Tests

Catalytic tests were made in a U-tube glass reactor of a diameter of 20 mm. First, 0.2 g of catalyst, of particles size between 500 and 800 mm, was placed on the glass frit. The heated parts of the reactor before and after the catalyst layer were filled by SiC chips. The reaction stream contained 0.6 vol.% of *n*-pentane, 6.3 vol.% of He, 19.5 vol.%. of O_2, and the rest was nitrogen. Total flow of the mixture was 30 ml/min. Brooks mass flow controllers were used to control the air and helium streams. The outlet of the reactor prior to analysis was kept at a temperature between 140 and 150°C. There was no detectable conversion of *n*-pentane in absence of a catalyst, provided the whole reactor was filled with SiC particles.

The inlet and the outlet gas streams were analysed by an on-line gas chromatograph equipped with a TCD detector on TENAX and Porapak Q columns (Altech Associates, Inc.), running under temperature program from 70 to 240°C. The outlet of the reactor prior to analysis was kept at about 150°C to prevent condensation of products.

The catalysts were pretreated with the reaction mixture according to a standard procedure consisting of a slow increase of temperature (about 5°C/min) up to 400°C, maintaining this temperature for 20 h, and subsequently decreasing it to 330°C. At this low temperature the molar conversion of *n*-pentane was always below 15%. The catalyst performance was measured after stabilising the system for about 2 h. Thus the total time-on-stream for an individual sample at the moment of the catalytic test run was about 40 h.

At the end of the catalytic test the reactor was cooled down to room temperature in the reaction mixture and the catalyst was taken out for analysis.

Calculation of the Molar Selectivity of MA and PA

The data of the catalyst performance, i.e., molar selectivity for MA and PA formation, were obtained on samples at the beginning of the equilibration process (compared to about 200 h necessary for full equilibration (9)) under conditions where the molar conversion of *n*-pentane was always equal to or lower than 15%. For evaluation of the catalyst performance the molar selectivity of MA or PA was calculated as follows:

Molar selectivity to MA, $S_{MA}(\%) = ((c_{MA})/(c_{C5})) \times 102$, and the molar selectivity of phthalic anhydride formation, $S_{PA}(\%) = ((2 \times c_{PA})/(c_{C5})) \times 102$.

In these expressions, c_{C5} is the amount of *n*-pentane transformed, i.e., moles of *n*-pentane in the inlet minus moles of *n*-pentane in the outlet stream (mole *n*-pentane per ml), and c_{MA} and c_{PA} the amounts of MA or PA produced (mole MA or PA per ml of the outlet gas mixture), respectively.

RESULTS

Preparation of Precursors

Precursor A

After about 2 h of mixing the equimolar solutions of isobutyl alkoxide and phosphoric acid in a water–isobutanol solvent a yellowish solid was formed. Under continuous stirring at room temperature, a very dense suspension with a colour varying from yellow (A[0]) to dark green (A[7]) was obtained.

Precursor Bo

The Bo[0] sample stayed yellow during the reflux of A[0] precursor in octane. In the other preparations (Bo[1] to Bo[4]), the colour of the suspension under reflux turned from yellow to black after 3 h for Bo[2] and about 5 h for Bo[1], Bo[3], and Bo[4]. The final isolated precursors Bo[1] to Bo[4] were dark brown. After refluxing the pure $VOPO_4 \cdot 2H_2O$ only a slight change of colour (from yellow to yellow-green) was observed.

Precursor Bi

Substantial differences were observed during preparation using precursors A with low (samples A[0]–A[3]) or high (A[4]–A[7]) content of water and accordingly the samples prepared into the reductive media were further divided in the following subgroups:

(i) Precursors Bi[0]–Bi[3]. These precursors were formed in the form of a blue solid by slow precipitation (about 6–8 h) from a dark green solution obtained in these preparations after about 1.5 h of reflux. Accordingly these are referred to as precursors Bi "via solution."

(ii) Precursors Bi[4]–Bi[7]. No apparent dissolution of the solid was observed by starting from precursors A with a high water content. Instead, the colour of the dispersed solid turned during the first two hours of reflux from yellow-green into pale blue and then did not change during the rest of the time of the reflux. These samples are further referred to in the text as precursors Bi prepared "via solid."

Preparation of Catalysts C

Precursors B were pretreated under reaction conditions by a standard procedure (see catalytic test). At the end of the catalytic test, i.e., after about 40 h on stream, the reactor was cooled to room temperature in the reaction mixture and the sample was taken out. Samples prepared from precursors Bo are denoted Co, samples prepared from precursors Bi are denoted Ci.

Characterisation of the Prepared Samples

(a) Chemical Analysis

Results for Precursors A, Bo, and Bi are presented in Tables 1, 2, and Fig. 2. All prepared materials presented only a small excess of phosphorus in the bulk ((P/V) bulk atomic ratio of about 1.05). The amount of organic material decreased with the amount of water added.

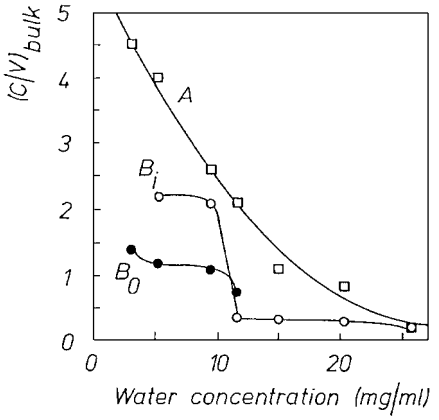

FIG. 2. Bulk atomic ratio of carbon to vanadium (C/V) bulk of precursors A, Bo, and Bi vs concentration of water in a water–isobutanol solution used for preparation of Precursors A. C/V bulk is the atomic ratio of carbon to vanadium as observed by a chemical analysis. A, Bo, and Bi in the figure indicate the type of precursor.

(b) Manganometric Titration

Results are presented in Table 1. The average oxidation state of vanadium in precursors A[0] to A[3] was five, and a small amount of vanadium with lower oxidation state was observed for A[4] to A[7] (average oxidation state about 4.8). After formation of precursors B, in either isobutanol or octane, the oxidation state of vanadium was 4, with the exception of sample Bo[0], where the oxidation state was about 4.5. No reduction of vanadium (V) was indicated after reflux of $VOPO_4 \cdot 2H_2O$ in octane.

The oxidation state of vanadium in Co[0] to Co[4] and Ci[3] and Ci[4] samples was found to be higher (average oxidation state about 4.5) than in samples Ci[5] to Ci[7], with an average oxidation state of 4.1 to 4.25 (see Table 3).

TABLE 2

Characterisation of the Chemical Composition of Precursors B and Their Specific Surface Areas

	Bo			Bi		
Sample	$(P/V)_b$	$(C/V)_b$	S_{BET} (m^2/g)	$(P/V)_b$	$(C/V)_b$	S_{BET} (m^2/g)
0	1.06	0.91	14.0			19.9
1	1.04	1.4	56.9			19.3
2	1.05	1.2	48.4	1.03	2.2	17.9
3	1.02	1.1	40.0	1.03	2.1	19.2
4	1.03	0.75	41.9	1.05	0.39	36.3
5				1.05	0.32	36.9
6				1.04	0.30	36.4
7				1.04	0.22	22.0

Note. $(P/V)_b$ is the bulk atomic ratio of carbon and vanadium as obtained by chemical analysis, $(C/V)_b$ is the bulk atomic ratio of carbon and vanadium as obtained by chemical analysis, and S_{BET} is the specific surface area obtained by BET measurement.

TABLE 3

Specific Surface Area of Samples C and Their Catalytic Activity

Sample name	S_{BET} (m^2/g)	Conversion of *n*-pentane (%)	MA selectivity (%)	PA selectivity (%)	Structural defects evaluation[a]	V^{n+b}
Co[1]	27.3	10.1	22	none	S + L	4.6
Co[2]	20	10.5	17.5	none	S + L	4.4
Co[3]	24.4	9.9	18.7	none	S + L	4.5
Co[4]	12.9	11.1	19	none	S + L	4.5
Ci[2]	14.9	11.7	5.6	none	L	4.25
Ci[3]	16.9	12.8	5.6	none	L	4.15
Ci[4]	26.3	15.6	24	4.8	O	4.1
Ci[6]	23.7	12.7	31	4.6	O	4.15
Ci[7]	19.0	12.4	26	9.6	O	4.05

[a] Structural defects evaluation: (S + L), both short and long range defects; L, long range defects; S, short range ordered structure; O, both short and long range order.

[b] V^{n+} is the bulk average oxidation state of vanadium.

(c) BET Specific Surface Areas and Porosity

Precursor A. Decomposition of the blue-green precursors into black material was observed during evacuation of the sample at 115°C. Consequently, no measurements were made on these samples.

Precursor Bo. The specific surface areas ranged from 57 to about 40 m^2/g for Bo[1] to Bo[4] samples (see Table 3). Results of the pore size distribution indicated the presence of pores with a diameter between 30 to 100 Å, with the amount of the small pores decreasing with amounts of water used in precursor A preparation.

Precursor Bi. The specific surface area of samples Bi[0] to Bi[3] is lower (about 19 m^2/g) than those of samples Bi[4] to Bi[7] (about 36 m^2/g) with the exception of sample Bi[7] (22 m^2/g) (see Table 2). Results of pore size distribution displayed a narrow pore size distribution with pore size diameter around 40 Å and systematic steep decrease of their volume from samples Bi[0] to Bi[6]. Pores in the 50–100 Å region were completely missing on sample Bi[7].

Samples C. Results are presented in Table 3. The specific surface area of samples after the catalytic test was substantially lower than that of the corresponding precursors Bo or Bi used for the test. No pores of a diameter below 100 Å were observed in Co or Ci samples.

(d) XRD Analysis

Precursor A. The results are presented in Fig. 3. The solid formed by preparation without any water (sample A[0]) has been identified as $VOPO_4 \cdot nC_4H_9OH$, by analogy to the group of previously described samples containing other C_3 or C_4 aliphatic alcohols (16). The position of the (001) reflection indicates an interlayer distance of 14.6 Å due to the intercalated isobutanol molecules. By increasing the amount of water in the preparation, the basal spacing decreases from about 14.6 Å for sample A[0] to about 7.1 Å for sample A[7]. Samples A[1] and A[2] display an intermediate structure between A[0] and A[7], with a broadening of the band at the position of the (001) reflection of $VOPO_4 \cdot nC_4H_9OH$ for A[0] and formation of an additional very intense and sharp peak at a 2θ value of about 28°, which could be assigned to the (002) reflection of $VOPO_4$ monohydrate. This last peak decreases in intensity from A[1] to A[6], suggesting that the layered structure is still similar to $VOPO_4$ monohydrate or dihydrate. Sample A[3] displayed a smaller structural order. The position of the band at lower 2θ for samples A[2] to A[6] shows a basal spacing of about 6.7 Å, higher than in $VOPO_4 \cdot H_2O$ (6.3 Å). Sample A[7] shows a basal spacing of about 7.1 Å, still less than the $VOPO_4$-dihydrate (with about 7.4 Å). The XRD spectra of sample A[7] showing a d spacing of about 7.12 Å (strong) and 3.5 and 3.04 Å (weak bands) clearly indicate the presence of $VOH_xPO_4 \cdot yH_2O$ phase (9, 20) in samples with higher amounts of water.

Precursor Bo. The XRD results are presented in Fig. 4. Sample Bo[0] presents a crystalline structure, quite different from the rest of the samples of the group Bo[1] to Bo[3]. These last samples, which are principally amorphous, display only a broad low intensity XRD reflection at $2\theta = 28.5°$. The position of this band coincides with the position of the most intensive (204) reflection of $(VO)_2P_2O_7$. We note that this species was obtained without calcination of the precursor at higher temperature.

Precursor Bi. The XRD spectra of the Bi precursors are presented in Fig. 5. They show a systematic change from amorphous (Bi[0]) to highly crystalline structure (Bi[7]) but with some discontinuity between the group constituted of the samples Bi[0]–Bi[3] and that of Bi[4]–Bi[7]. The group of amorphous samples, Bi[0] to Bi[3], displays only one

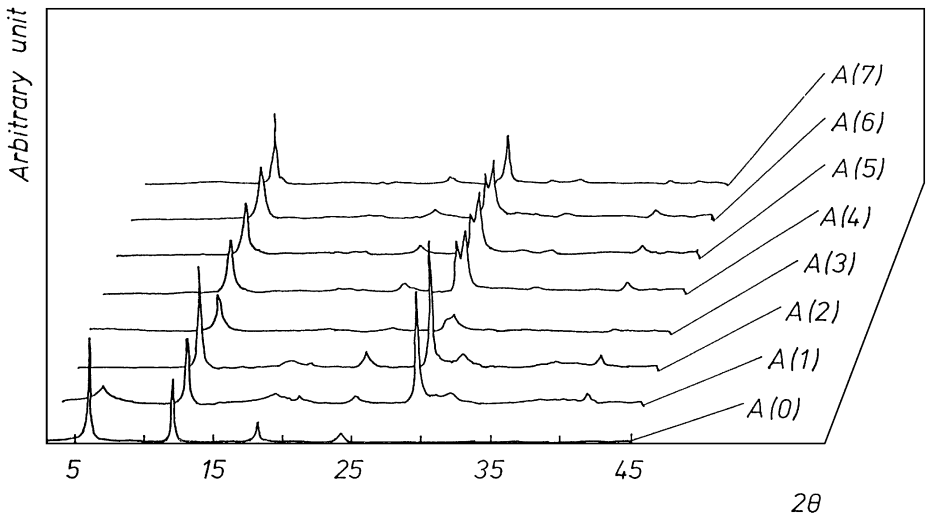

FIG. 3. XRD spectra of precursors A.

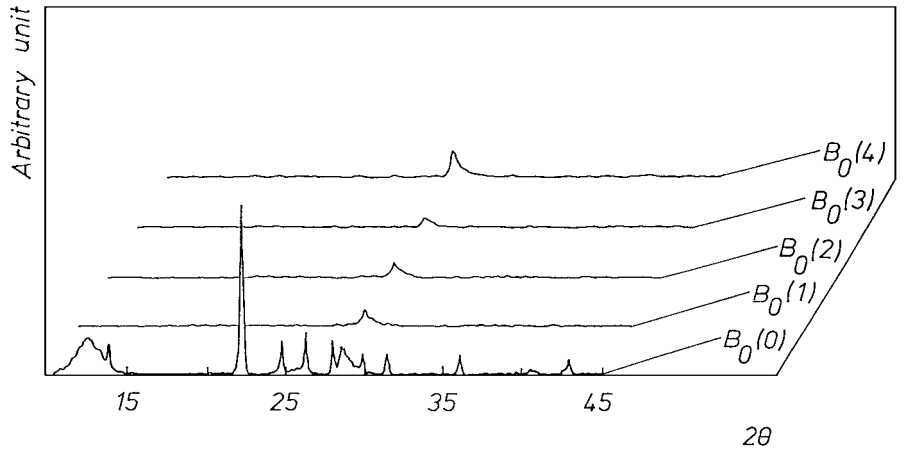

FIG. 4. XRD spectra of precursors Bo.

broad band with 2θ at 30.4°. This band can be assigned to $VOHPO_4 \cdot 1/2H_2O$. The intensity of this band decreases from Bi[3] to Bi[0]. The fact that the line at $2\theta = 15.5°$ is missing indicates a high disorder along the (010) plane (11). These samples present a very defective structure. The group of samples Bi[4] to Bi[7] corresponds to the well-developed structure of $VOHPO_4 \cdot 1/2H_2O$. The broadening of the (010) band ($2\theta = 15.5°$) and changes in the (010)/(202) intensity ratio (bands at $2\theta = 15.5°$ and $2q = 30.4°$) is typical of samples prepared in organic media (12).

Samples C. In accordance with a very short equilibration period, the samples did not contain a well-developed crystalline $(VO)_2P_2O_7$ structure typical of fully equilibrated VPO catalysts. Ci[2] and Ci[3] and samples Co[1] to Co[3] were very amorphous. Only a badly resolved reflection at the position of the (042) line was observed. For the group of samples Ci[4] to Ci[7], lines typical of $(VO)_2P_2O_7$ were observed. The XRD results for these groups of samples are exemplified by samples Ci[7] and Co[3] and they are presented in Fig. 6.

(e) FTIR Spectroscopy

The FTIR spectra are presented in Figs. 7–9 and the assignment of the bands in Tables 4 and 5.

Precursor A. Only small differences were found among the spectra. The only evident variations concern the H_2O vibration band, showing a systematic shift from a broader band at about 1620 cm^{-1} in sample A[0] to a pair of bands at about 1614 and 1640 cm^{-1} for sample A[7].

Precursor Bo. Results are presented in Fig. 7. For sample Bo[0] several intense and well-resolved bands at about 1176, 1095, 720, and 780 cm^{-1} were observed. On the other hand the IR spectra of samples Bo[1]–Bo[4] display a broad unresolved band between ca. 520 and 1400 cm^{-1}, with a maximum at about 1085 cm^{-1} and several very diffuse low intensity bands in the 400–700 cm^{-1} region. All these bands can be tentatively assigned to a very defective structure of vanadyl phosphate (12, 15).

Precursor Bi. Results are presented in Fig. 8. The assignment of the IR bands for the Bi[0]–Bi[3] samples

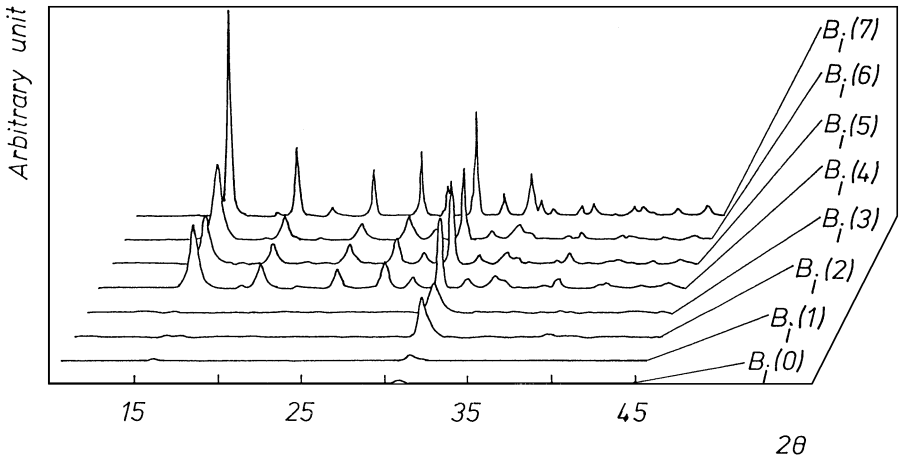

FIG. 5. XRD spectra of precursors Bi.

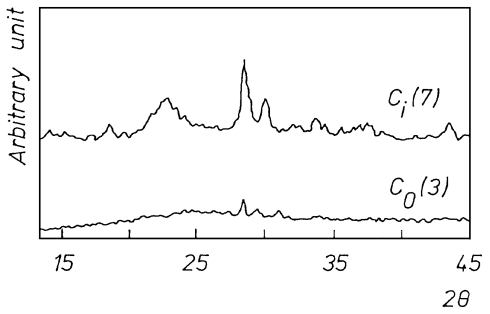

FIG. 6. XRD spectra of precursors Co[3] and Ci[7].

(exemplified by sample Bi[0]), Bi[4]–Bi[7]) is presented in Table 4.

Comparing both types of Bi samples it could be summarised that the via solution prepared samples differ in the following structural features:

(i) bands assigned to POH (δ_{ip} POH at 1133 cm^{-1} and νP-(OH) at 933 cm^{-1}) are suppressed;
(ii) the group of IR bands belonging to the O–P–O structure (δOPO at 413, 482, 534, and 550 cm^{-1}) are very broad and of a very low intensity.
(iii) A band at 686 cm^{-1} assigned to the coordinated water molecules is missing or badly developed and accompanied by a parallel shift in the position of the ωH_2O band.

Additional bands were found in the spectra of Bi[0] to Bi[3] samples at 1474, 1399, and 1372 cm^{-1} and at 2867 cm^{-1}. These bands were observed also but with much lower intensity in the Bi[4] to Bi[7] samples. These bands have not been assigned to the $VOHPO_4 \cdot 1/2H_2O$ structure.

Samples C. Results are presented in Fig. 9 with the assignment of the IR bands for these samples indicated in Table 5.

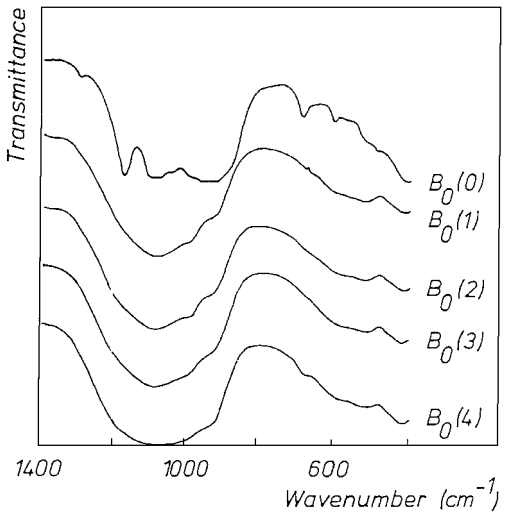

FIG. 7. FTIR spectra of precursors Bo at the region of 1400 to 400 cm^{-1}.

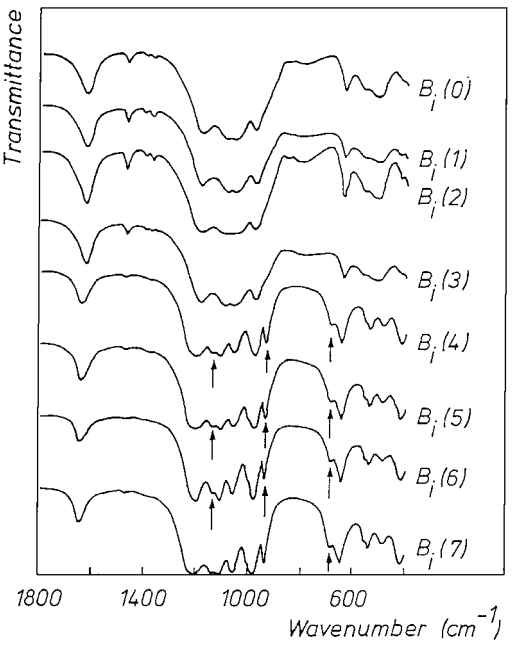

FIG. 8. FTIR spectra of precursors Bi at the region of 1800 to 400 cm^{-1}.

Sample Co. The IR results for the samples Co[1] to Co[4] (exemplified here using the spectrum of sample Co[2]) show a very broad unresolved band between 800 and 1400 cm^{-1}. Most of the features typical of a developed $(VO)_2P_2O_7$ structure are missing. The very broad band could be tentatively assigned to a defective structure of a vanadyl phosphate.

TABLE 4

IR Absorption Bands of Samples Bi and $VOHPO_4 \cdot 1/2H_2O$ (12) and Their Assignment

$VOHPO_4 \cdot 1/2\ H_2O$	Attribution	Bi [O]	Bi[7]
3590	$\nu_a\ OH_2$	3580	3590
3370	$\nu_s\ OH_2$	3410 (B)	3370
1645	$\delta\ H_2O$	1629	1643
1132	δ_{ip} POH	M	1133
1194		1183	1198
1103	$\nu_{as}\ PO_3$	1090	1106
1050		1054	1054
976	ν V=O ($+\nu_s PO_3$)	978	977
930	ν P-(OH)	M	933
686	$\varpi\ H_2O$	M	686
641	δ_{oop} POH	637	642
548		560	550
531	δ OPO	(w,B)	534
483		(w,B)	483
416		(w,B)	413

Note. The notation for the IR bands used in the table is in the form presented in a Ref. (12). M, band is missing; w, weak band; B, broad band.

TABLE 5

IR Absorption Bands of Sample C and $(VO)_2P_2O_7$ and Their Assignment (12)

$(VO)_2P_2O_7$ (cm^{-1})	Attribution	Ci[3] (cm^{-1})	Ci[7] (cm^{-1})	Co[2] (cm^{-1})	VPO-N (cm^{-1})	VPO-S (cm^{-1})
1235	ν_{as} PO_3	(w,B)	1239	(w,B)	1241	1239 (B)
1220		(w,B)	1220		1220	
1140		1150	1143	1135 (B)	1139	1142
1115	ν_{as} PO_3	(w,B)			1110	
1095	ν_s PO_3	1030	1090	1040	1095	1034
966	νV=O		971	990 (B)	971	971
960	ν_{as} POP	950	960	M	920	935
792	νV=O	M	790	M	794	M
740	ν_s POP	M	745	770	743	766
627		630 (w,B)	634		633	633
577	δOPO	568 (w,B)	578	576 (w,B)	579	576
504		510 (w,B)	511	511 (w,B)	512	514
420		420 (w,B)	423		423	422

Note. M, band is missing; w, weak band; B, broad band. VPO-N, VPO-S (8), results of the previous paper on samples prepared via full development of the precursor A (VPO-N) or directly from solution (VPO-S).

Sample Ci. A difference between the group constituted of samples Ci[0] to Ci[3] (exemplified here using the spectrum of sample Ci[3]) and that of Ci[4] to Ci[7] (exemplified here using the spectrum of sample Ci[7]) is observed after the catalytic test.

(i) The spectra of the Ci[0] to Ci[3] catalysts are poorly resolved and display a broad band in the 800 to 1400 cm^{-1} range.

(ii) The Ci[4] to Ci[7] samples display most of the features typical of $(VO)_2P_2O_7$ structure. Bands at 790 and 743 cm^{-1}, associated with the links between layers, are clearly detected.

(f) XPS Analysis

XPS results for Ci and Co samples are shown in Table 6.

Samples Co. Three samples were analysed, Co[0], Co[1], and Co[2]. They show similar XPS P/Si, O/Si, and C/Si surface atomic ratios. The XPS C/P surface atomic ratio values increase slightly from Co[0] to Co[2]. A decrease of the XPS V/Si atomic ratio for sample Co[1] to nearly half of the value observed for samples Co[0] and Co[2] is noted. The XPS P/V and C/V atomic ratios are significantly higher for sample Co[1].

Samples Ci. The XPS P/Si, V/Si, and O/Si XPS surface atomic ratios showed a slightly higher value for samples Ci[4] to Ci[7] compared to Ci[2] and Ci[3]. On the contrary, the C/Si decreases from Ci[2] to sample Ci[7]. XPS surface atomic ratio of C/V displayed substantially higher values for Ci[2] and Ci[3] samples than for Ci[4] to Ci[7]. The value of the XPS P/V atomic ratio observed was nearly similar for all Ci samples. Only one vanadium species with BE at 517.4 eV has been observed for the samples of the Ci series. The same BE value was observed by Cornaglia (21) and Zazhigalov (22). It was found to be independent

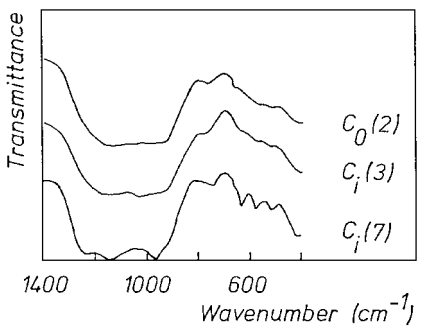

FIG. 9. FTIR spectra of samples Co[2], Ci[3], and Ci[7] at the region of 1400 to 400 cm^{-1}.

TABLE 6

XPS Results of Samples Ci[2]–Ci[7] and Co[0]–Co[2]

	XPS atomic ratio						
Sample	P/V	P/Si	V/Si	C/P	C/V	C/Si	O/Si
Ci[2]	1.59	0.46	0.29	1.32	2.10	0.61	2.00
Ci[3]	1.55	0.45	0.29	1.38	2.13	0.62	2.00
Ci[4]	1.52	0.47	0.31	1.04	1.59	0.49	2.12
Ci[6]	1.56	0.50	0.32	0.94	1.47	0.47	2.10
Ci[7]	1.58	0.49	0.31	0.92	1.45	0.45	2.13
Co[0]	1.75	0.49	0.28	0.83	1.46	0.41	2.22
Co[1]	3.00	0.48	0.16	1.12	3.37	0.54	2.22
Co[2]	1.55	0.45	0.29	1.18	1.82	0.53	2.12

Note. Two decimal numbers are used for the XPS atomic ratios. A/B values in the table: XPS atomic ratio calculated by the method explained at the experimental part.

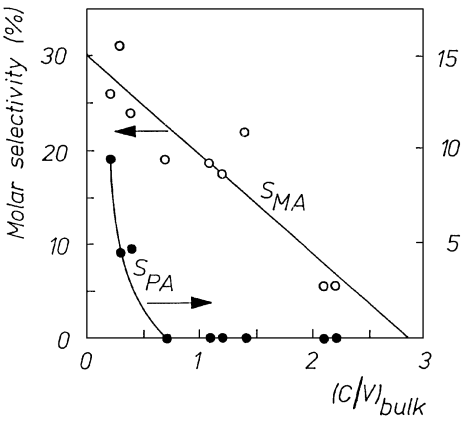

FIG. 10. Selectivity to maleic anhydride (SMA) or phthalic anhydride (SPA) vs atomic ration of carbon to vanadium in the bulk (C/V bulk) at the precursor B, used for the catalytic test.

from both the preparation method used and the catalyst time on stream. This value of the binding energy is usually associated with V^{4+} (19).

Two different vanadia species, having BE of about 518.5 and 517.4 eV were observed in the Co samples. In a first attempt, it is logical to associate the higher BE value with a higher oxidation state of vanadia, V^{5+}, and the lower value to V^{4+}. Nevertheless, by comparing these values with the BE value observed in a pure V_2O_5 standard, the higher BE should be attributed to a shift of the binding energy of the V2p3/2 for both V^{5+} and V^{4+} in samples Co. This shift is of about 1.1 eV.

Catalytic Activity

Samples Co. The conversion at 330°C and the selectivity to anhydrides are shown in Table 3. Except for sample Co[0] showing substantially lower selectivity, the rest of the Co samples, i.e., Co[1] to Co[4], were similar in selectivity to MA. No PA was observed for these samples.

Samples Ci. The results are presented in Table 3. The conversion of *n*-pentane of the Ci samples showed a rough correlation with the value of the specific surface areas after the catalytic test. A lower selectivity to MA formation was observed in the Ci via solution (i.e., Ci[2] and Ci[3]) samples). Formation of phthalic anhydride was observed exclusively over samples via solid (i.e., Ci[4] to Ci[7]), with the highest selectivity in PA for Ci[7].

Figure 10 plots the selectivity as a function of the amount of intercalated organic compounds in the precursors B used for the catalytic tests, expressed as the C/V bulk atomic ratio. A linear increase of the MA selectivity with a decreasing amount of intercalated organic material can be observed. On the other hand, PA is formed only when the C/V ratio is low and the ratio of the selectivities to PA and MA changes abruptly at low C/V ratios.

DISCUSSION

The processes taking place during the formation of the precursors and their influence on the selectivity of the catalytic process will be discussed.

Formation of Precursor A

The A[0] sample prepared in anhydrous conditions corresponds to the $VOPO_4$–isobutanol intercalate, with an interlayer distance of 14.6 Å intermediate between the propanol (14.39 Å) and *n*-butanol intercalate (17.96 Å) (16) near the value for propanol intercalate as the branching methyl substituent generally contributes less to the increase of the interlayer distance (16).

For the other samples, the IR and XRD results and calculation of the amount of alcohol molecules in the samples pointed to the formation of a series of a $VOPO_4$-mixed water–isobutanol intercalated with the water content regularly increasing in the sequence from A[0] to A[7]. Due to the easy exchange of alcohol and water molecules in the interlayer position (16, 17), it could be assumed that the water–alcohol equilibrium is established under the preparation conditions.

The distortion of the (001) band of the $VOPO_4$ alcohol intercalate and the decrease of the basal spacing already observed with the A[2] sample, leading ultimately to about the value typical of $VOPO_4 \cdot 2H_2O$, seems to indicate that in samples A[1] to A[7] the water molecules successfully compete with isobutanol for the bonding to the (VO_5) unit. Actually the additional line at $2\theta = 28.5°$ in samples A[1] to A[7] could be assigned to the (002) line of $VOPO_4 \cdot H_2O$. Thus, our results strongly suggest that the interlayer distance is mostly related to the strongly bonded water molecules as in $VOPO_4$ hydrates and the alcohol molecules could move along the layers.

Thus the series of A[0] to A[7] presents a complex sequence of mixed water–isobutanol intercalates, starting from a nearly pure isobutanol (sample A[0]), forming a monohydrate when increasing the water content (mostly samples A[1] and A[2]), and leading to the formation of $V_{4.8}OH_xPO_4$ intercalate, accommodating small amounts of slightly reduced vanadium in the structure (samples A[4] to A[7]), as supported by the results of manganometric titration.

Transformation of Precursor A into B

As precursor A contains mostly vanadium in a high oxidation state, namely 5^+ for samples A[0] to A[3] or about 4.8^+ for samples A[4] to A[7], the process of vanadium reduction to vanadium (IV) found in precursors B occurs mostly during the reflux of samples A.

Reduction in n-Octane (Sample Bo)

The vanadium (5^+) in the $VOPO_4$ mixed water–isobutanol intercalate is very sensitive to reduction. After

heating in an inert media (*n*-octane) vanadium V(5^+) is reduced to V(4^+).

No reduction was indicated for $VOPO_4 \cdot 2H_2O$. It implies that the isobutanol molecules present in the solid structure should serve as a reducing agent for this reaction. As will be discussed later, such a process produces highly amorphous samples.

Reduction in Isobutanol Media (Samples Bi)

The reduction process in isobutanol could occur both in a homogeneous solution and in a solid phase. Accordingly, either the intercalated isobutanol molecules or the isobutanol present as solvent could serve as reducing agent.

Transformation of the partially soluble precursor A into a precipitate of the final product, $VOHPO_4 \cdot 1/2H_2O$, seems to be very dependent on the amounts of precursor A and isobutanol used. In fact, a precise balance between the amount of solid vs isobutanol volume is critical for observing the reaction via solid or via solution. This has been confirmed in experiments using the same amount of precursor A as in the results presented but with 3 times more isobutanol (120 ml instead of 40 ml). In this case, all the samples of the A series were completely dissolved during reflux. Due to the difference of the reduction process via solution or via solid, these two procedures will be discussed separately.

Reduction in Homogeneous Solution ("via Solution")

This concerns the preparation of precursors Bi[0]–Bi[3]. By starting from a precursor A which contains a low amount of water, highly defective $VOHPO_4 \cdot 1/2H_2O$ samples retaining a substantial amount of organic species are formed by slow precipitation under reflux. The conditions for developing a regular $VOHPO_4 \cdot 1/2H_2O$ are severely limited because the amount of water in the produced precursor Bi is limited to the amount already present in precursor A, and produced precursor B contains a high amount of organic material.

Reduction in Solid Phase ("via Solid")

This concerns the preparation of precursors Bi[4] to Bi[7]. It has been shown, by decomposition of the mixed intercalates in octane, that the isobutanol molecules trapped inside the $VOPO_4$ structure are able to play the role of reducing agent with respect to the vanadium present. Using isobutanol as a medium, the precursors formed (Bi[4] to Bi[7]) contained low amounts of organic species and had a highly ordered structure. We suggest that, under such conditions, a process of reductive intercalation as described by Jacobson *et al.* (23) operates. These authors showed that the structure of $VOPO_4 \cdot 2H_2O$ could be, during reduction, stabilised by compensation for the lower charge of the vanadium cation by intercalating mono- or divalent cations, forming $VOM_xPO_4 \cdot 2H_2O$ and thus preserving the layered structure of the starting vanadyl phosphate up to a very high reduction level of V(5^+) to V(4^+). Under similar conditions, and using hydroquinone in acetone solution as a reducing agent, a series of $VOH_xPO_4 \cdot yH_2O$ with x changing from 0.3 to 1.0 were prepared by Zima *et al.* (20).

Accordingly we suggest that in the via solid conditions, the reduction is due at least partially to such a reductive intercalation process. The reduction probably starts using the isobutanol molecules already present in the mixed intercalate (precursor A) and the lower charge of the vanadium is partially compensated by a proton, probably coming from the water present. During this reduction process, an intermediate corresponding to a sort of $VOH_xPO_4 \cdot nH_2O$ is probably formed and, consequently, the reduction actually proceeds to some extent in the layered structure of $VOPO_4 \cdot nH_2O$, thus providing for expulsion of most of the oxidised organic products from the solid and accordingly producing precursors B with a low C/V value. As mentioned previously, this process would occur preferentially in the cases in which the H_2O molecules are strongly bonded at the $VOPO_4$ layered structure and thanks to the free movement of the organic molecules. This process facilitates the formation of a highly ordered structure of the $VOHPO_4 \cdot 1/2H_2O$, as found principally in the Bi[7] preparation.

Obviously, the reductive intercalation is not realised in an inert media of isooctane and thus the Bo samples retain a substantially higher amount of organic residue (compared to Bi[4] to Bi[7], Table 2) and Bo gives highly amorphous structures.

An attempt to characterise the level of the structural order of the layered structures of the vanadyl phosphates is given considering that these defects correspond generally to two categories, i.e., long range or short range defects. The idea is to distinguish roughly between the disorder effecting interlayer connections of the layers of the crystal lattice (long range defects) and the local disorder around the vanadium atoms (short range defects); see also, e.g., (11) and (12) using a similar concept.

The general structural features of these two categories were as follows:

(i) long range defects showing destruction of links between vanadyl phosphate layers indicated by broadening and eventually missing of the XRD bands and suggested by the missing of IR bands of δ_{ip} P–OH and νP–OH at 1135 and 927 cm^{-1}, respectively, and of ωH_2O at 686 cm^{-1}.

(ii) short range defects exhibiting distortions inside the $VOPO_4$ sheets. In this category one has to consider broad bands or bands which cannot be distinguished from other IR bands of vanadyl phosphate molecules in the 1400–400 cm^{-1} region.

Using this approach the structural characteristics of the samples prepared in various preparation routes were characterised as follows:

(i) Precursors Bo[1]–Bo[4] display a high extent of defects, both of the long range and of the short range character.

(ii) Precursors Bi prepared via solution (Bi[1]–Bi[3]) contain mostly long range defects (see Fig. 5), but the short range order is mostly retained.

Precursors Bi prepared via solid (Bi[4]–Bi[7]), displayed both short and long range orders.

By comparing these structural characteristics with the amount of the organic species present in the precursors B, and expressed as the C/V value, the general trend between the efficiency of fragments elimination of the reducing agent during the formation of precursor from precursor A and the extent of their structural defects is also suggested.

Transformation of Precursors B under Reaction Conditions

It was postulated by Bordes (17) that the $VOHPO_4 \cdot 1/2H_2O$ precursor is transformed into $(VO)_2P_2O_7$, which is the active phase, by a topotactic solid state transformation. Recently, it has been argued by several authors (6, 9) that such a topotactic transformation is unlikely and that the transformation is going through an amorphous phase. Nevertheless there seems to be a general consensus that the morphology of the $VOHPO_4 \cdot 1/2H_2O$ precursors (precursor B in our notation) and defects in their structure are transcribed to a high extent into the structure of the catalyst (12, 21). This could be attributed to the structural relations between the structure of the precursor B and that of the VPO catalyst at the low extent of equilibration at the catalytic conditions. As shown clearly by Alboreti *et al.* (9), the equilibration process reflects a slow formation of the well crystalline $(VO)_2P_2O_7$ from a precursor of lower crystallinity and needs for its completion up to 200 hours.

Our results are in favour of a mechanism preserving in the catalysts the level of structural disorder present in the VPO precursor. Namely the general structural features classified as long and short range order observed for precursors B mostly apply also for samples C, i.e., for catalysts after short equilibration (only 40 hours). Accordingly no apparent crystal order was developed starting from the highly amorphous precursors of Co type and a good correlation exists between the order level characterised in detail in the precursors Bi and indicated in the Ci samples.

We do not have enough arguments to attribute with certainty the additional vanadium species at a higher oxidation state (BE of 518.5 eV) observed in Co samples. It could be tentatively attributed to the increase of the electropositive character of surface-bound vanadium in the highly amorphous environment (compare Horvath *et al.* (24)).

Evaluation of the Relationship between Structural Parameters of a Catalyst and Its Catalytic Performance

In our previous work (8), we showed that the formation of maleic and phthalic anhydrides could be controlled by varying the experimental conditions during precursor preparation. Nevertheless difference in the P/V ratio of the analysed samples makes the arguments less convincing. On the contrary, in the present work, samples are characterised by the same and nearly stoichiometric P/V bulk atomic ratio. The development of the $VOHPO_4 \cdot 1/2H_2O$ (precursor B) was then controlled principally by the amount of water added during the preparation of the precursors. The samples then differed by the amount of intercalated organic material as shown by the changes of the C/V values.

Clearly two selectivity patterns are observed:

(i) MA was the only product of selective oxidation over catalysts produced from Bo or Bi by the via solution preparation route, i.e., starting from precursor A with a low content of water, both displaying no or only short range order (see Table 3);

(ii) Catalysts obtained by the via solid route in which both short and long range orders are present, produced by *n*-pentane oxidation both MA and PA.

Formation of MA

The linear increase of selectivity to MA with the decreasing amount of organic material, expressed by the C/V value (Fig. 10), reflects the details in the change in structural order caused by the presence of the intercalated organic species in precursor B. It should be mentioned that this correlation obviously applies for all types of prepared catalysts, despite the qualitatively different character of the structural defects of the various Bo and Bi precursors.

The above correlation found in the present work is supported by results of Cornaglia *et al.* (25) showing an increase of butane transformation into MA over VPO catalysts with a higher structural order. This increase of structural order was accompanied by development of strong acidic centers which are made responsible for the increase in the selectivity to MA. Nevertheless, our results also show that in the oxidation of *n*-pentane, MA can be produced even on VPO structures exhibiting an important level of structural disorder.

Formation of PA

By comparing PA and MA selectivities (Fig. 10) it can be observed that the process of PA formation displays a substantially different sensitivity to the nature of the structural defects of the catalyst. For the PA formation, a more ordered structure of the crystalline phases of the VPO catalysts is necessary, such as in the Ci samples prepared from Bi[4] to Bi[7] precursors.

It could be suggested that both short and long range structural orders are necessary to create the surface topology of the complex active centres with an optimal distribution of the individual active sites (strongly acidic centres among

others) to allow the concerted process with an extremely high demand on the availability of all the specific active sites in a proper topological order leading to PA formation. Such a complex structure could, e.g., look like a tridimensional active site as proposed by Ebner (6). But this hypothesis needs further confirmation and at this state of the study this is only a speculation.

CONCLUSIONS

It has been shown that, by varying the water/isobutanol ratio in the preparation solution, the formation of the $VOHPO_4 \cdot 1/2H_2O$ precursor could be accomplished by a solid state reaction by a reductive intercalation. This produces a highly ordered crystalline material with a limited amount of organic products retained in the structure of the produced precursor.

By comparing between them the catalytic performances over such prepared VPO catalysts, and using catalysts prepared from highly disordered precursors produced by a process using the intercalated isobutanol as the reducing agent it in an inert media, or by precipitation from a solution with a low amount of water present, we suggest that both short and long range structural orders are necessary for PA formation by oxidation of *n*-pentane over VPO catalysts.

It could be concluded that the previous suggestions (8, 9) about the correlation between the structural order of the $(VO)_2P_2O_7$ and PA formation under *n*-pentane oxidation is correct. The effect is independent from the process by which the disorder in the VPO catalyst is created, i.e., by varying the method of precursor preparation or the time for VPO catalyst equilibration.

ACKNOWLEDGMENTS

The stay of S. R. G. Carrazan was supported by the Direccion General de Investigaciones Cinetificas DGICYT (Programa FPU), Ministerio de Educacion y Ciencia de Espana, which is gratefully acknowledged. The Service de la Programmation de la Politique Scientifique (Belgium) is gratefully acknowledged for its Concerted Action grant, especially for the support of Z. Sobalik and P. Ruiz. The authors also thank Mr. M. Genet for his help in the XPS analyses. We acknowledge the support of the Belgian National Foundation for Scientific Research (FNRS) for financing the laboratory equipment used in this research.

REFERENCES

1. Centi, G., Gleaves, J. T., Golinelli, G., and Trifiro, F., *in* "III European Workshop Meeting New Developments in Selective Oxidation" (P. Ruiz and B. Delmon, Eds.), *Stud. Surf. Sci. Catal.* **72**, 231 (1992).
2. Centi, G., Trifiro, F., Ebner, J. R., and Franchetti, V. M., *Chem. Rev.* **88**, 55 (1988).
3. Cavani, F., Colombo, A., Giuntoli, F., Gobbi, E., Tvit, F., and Vazquez, D., *Catal. Today* **32**, 125 (1996).
4. Cavani, F., Colombo, A., Trifiro, F., Schulz, M. T. S., Volta, J. C., and Hutchings, G. J., *Catal. Lett.* **43**, 241 (1997).
5. Cavani, F., and Trifiro, F., *Appl. Catal. A-General* **157**, 195 (1997).
6. Ebner, J. R., and Thompson, M. R., *Catal. Today* **16**, 51 (1993).
7. Centi, G., *Catal. Today* **16**, 5 and 147 (1993).
8. Sobalik, Z., Gonzalez, S., and Ruiz, P., *in* "Preparation of Catalysts VI. Scientific bases for the Preparation of Heterogeneous Catalysts," *Stud. Surf. Sci. Catal.* **91**, 727 (1995).
9. Albonetti, S., Cavani, F., Trifiro, F., Venturoli, P., Calestani, G., Lopez Granados, M., and Fierro, J. L. G., *J. Catal.* **160**, 52 (1996).
10. Granados, M. L., Conesa, J. C., and Fernandez-Garcia, M. F., *J. Catal.* **141**, 671 (1993).
11. Cornaglia, L. M., Caspani, C., and Lombardo, E. A., *Appl. Catal.* **74**, 15 (1991).
12. Busca, G., Cavani, F., Centi, G., and Trifiro, F., *J. Catal.* **99**, 400 (1986).
13. Bradley, D. C., Mehrotra, R. C., and Gaur, D. P., "Metal Alkoxides." Academic Press, San Diego, 1978.
14. McMurdie, H., *Powder Diffraction* **1**, 98 (1986).
15. Ladwig, G., *Z. Anorg. Allg. Chem.* **338**, 266 (1865).
16. Benes, L., Votinsky, J., Kalousova, J., and Klikorka, *J. Inorg. Chim. Acta* **114**, 47 (1986).
17. Bordes, E., Courtine, P., and Johnson, J. W., *J. Solid State Chem.* **55**, 270 (1984).
18. R'Kha, C., Vandenborre, M., Livage, J., Prost, R., and Huard, E., *J. Solid State Chem.* **63**, 202 (1986).
19. Carrazan, S. R., Peres, C., Bernard, J. P., Ruwet, M., Ruiz, P., and Delmon, B., *J. Catal.* **158**, 452 (1996).
20. Zima, V., Benes, L., Votinsky, J., and Kalousov·, J., *Solid State Ionics* **82**, 33 (1995).
21. Cornaglia, L. M., Sanchez, C. A., and Lombardo, E. A., *Appl. Catal. A: General* **95**, 117 (1993).
22. Zazhigalov, V. A., Haber, J., Stoch, J., Pyatnitzkaya, A. I., Komashko, G. A., and Belousov, V. M., *Appl. Catal. A: General* **96**, 135 (1993).
23. Jacobson, A. J., Johnson, J. W., Brody, J. F., Scanlon, J. C., and Lewandowski, J. T., *Inorg. Chem.* **24**, 1782 (1985).
24. Horvart, B., Strutz, J., Geyer-Lippmann, J., and Horvart, E. G., *Z. Anorg. Allg. Chem.* **483**, 181 (1981).
25. Cornaglia, L. M., Lombardo, E. A., Anderson, J. A., and Fierro, J. L. G., *Appl. Catal.* **100**, 37 (1993).